ELSEVIER

Journal of Alloys and Compounds 356–357 (2003) 160–168

Journal of ALLOYS AND COMPOUNDS

www.elsevier.com/locate/jallcom

Adjustable magnetic interactions: the use of hydrogen as a tuning agent

B. Hjörvarsson[a,*], C. Chacon[a], H. Zabel[b], V. Leiner[b]

[a]*Uppsala University, Department of Physics, Box 530, S 751 21 Uppsala, Sweden*
[b]*Ruhr-Universität Bochum, Festkörperphysik, D-44780 Bochum, Germany*

Received 1 September 2002; accepted 31 December 2002

Abstract

The use of hydrogen to modify the electronic structure in magnetic thin films and heterostructures has opened new routes to tailor magnetic interactions in materials. The presence of hydrogen modifies the electronic structure of the host. Hydrogen can therefore be used to control the strength and character of magnetic interactions. This effect can be used to change the coupling strength in thin films, as well as selectively altering one of the constituents in artificial heterostructures. For example, the switching from antiferromagnetic to ferromagnetic order, and vice versa, has been demonstrated for exchange coupled magnetic superlattices. As the sign of the interlayer exchange coupling J' can be switched by the insertion of hydrogen, J' arbitrarily close to zero must be accessible. When $J'=0$, the exchange interaction between adjacent magnetic layers is completely suppressed. The heterostructure can then be taken to consist of a collection of quasi two-dimensional magnetic sheets, when the ferromagnetic layers are very thin. Consequently, the introduction of hydrogen can be viewed as a route to tune the dimensionality of these structures.

Keywords: Hydrogen; Thin films; Multilayers; Superlattices; Exchange coupling; Rare earth metals; Transition metals

1. Introduction

In an ideal experiment, all parameters and properties of the system can be determined. While changing one experimental variable and observing the invoked changes, a unique response would be obtained. This idealized version of the scientific endeavour is not often realized. One recent example, which is close to this idealized route, is the research on magnetic exchange coupling in artificial heterostructures. When ferromagnetic sheets are separated by a few monolayers (ML) of nonmagnetic material (spacer), the interlayer magnetic ordering can, for example, be either ferromagnetic (FM) or anti-ferromagnetic (AFM) depending on the thickness of the spacer [1]. When growing two samples with the same thickness of the spacer, but using different elements, different magnetic ground states can emerge. The electronic structure of the spacer is therefore equally important as its thickness for describing the interlayer exchange coupling (IEC). While temperature and external field can be varied continuously and reversibly (within a certain range), the thickness of the layers can only be obtained in discrete atomic steps through the preparation of a series of different samples. The same has been true for the electronic configuration of the spacer layers.

Absorption of hydrogen is known to alter many material properties [2–4]. In both transition (TM) and rare earth (RE) metals, this change can be viewed as resulting from a modification of the electronic structure through hybridisation, combined with a local lattice distortion. The changes are strongly linked to the hydrogen concentration, as revealed by, for example, conductivity measurements [4]. Hydrogen can therefore be viewed as a tool to modify the electronic structure, allowing tuning of different physical properties. In this perspective hydrogen (including D and T) is unique, no other elements can be reversibly inserted and removed in solid materials with the same ease.

Hydrogen can only be inserted and removed reversibly within the concentration range of a primary solid solution [2]. Hydrogen induced embrittlement and cracking accompanying the phase separation at higher concentrations usually limit the accessible reversibility range. Increasing the temperature of the sample partially solves this problem, as the terminal hydrogen solubility often increases with temperature. This approach, however, severely limits the possibilities of investigating the temperature dependence of the properties of interest.

*Corresponding author.
E-mail address: bjorgvin.hjorvarsson@fysik.uu.se (B. Hjörvarsson).

0925-8388/03/$ – see front matter
doi:10.1016/S0925-8388(03)00168-3

When the hydrogen absorbing material is confined in one or more dimensions, strong influence on the ordering of hydrogen is obtained [5]. Influence of the finite size is, e.g. manifested through spatial restrictions on the density fluctuations [6,7], and in the extreme limit the boundaries are directly affecting the absorption potential [7,8]. These effects open a route towards completely reversible hydrogen loading over a wide concentration and temperature ranges. However, the influence of the substrate must be regarded when discussing the hydrogen uptake of these artificial structures. One of the key assets in the current context is the strong adhesion of a film to the substrate [9]. This adhesion makes investigations of extremely thin layers possible, through preventing bending or cracking of the films. For example, layers can be loaded with hydrogen to high concentrations, causing strong tetragonal distortion of the unit cell of the host material. The broken symmetry will affect the resulting electronic structure and can also promote or hinder a change of site occupancy. The most extreme case of reversible loading described in the literature, is in Fe–V(001) superlattices. Hydrogen concentrations close to 1[1] were reversibly obtained in the V layers [10] through selective population of the octahedral *z* sites. In Fe–V(001) superlattices, the selective population can be described as a complete polarization of the dipolar strain field, associated with the occupation of octahedral sites [11,12]. An example of nonreversible loading is discussed by Rehm et al. [13] and Klose et al. [14]. A comprehensive discussion of the finite size and strain effects in thin films and superlattices is, e.g. found in Ref. [4] and references therein.

The most spectacular changes in the tuneable properties of thin films and superlattices are in the optical [15] and the magnetic [16,17] properties. Optical transmission of thin films can be changed by orders of magnitude by loading or removing hydrogen. The changes of the magnetic properties are as spectacular, albeit not directly observable by the naked eye. The strength of the magnetic interaction can be gradually weakened and the magnetic ordering can be removed upon hydrogen loading, ordering can be reversed (ferromagnetic to antiferromagnetic) and the repeat distance of magnetic helical spirals can be tuned [18].

Here we will give a brief review of the magnetic properties of thin films and superlattices and we will discuss the possibility of using hydrogen as a tuning agent. We will start with thin films, addressing changes in the inherent material properties as well as the effect of finite size and adhesion. Thereafter we will treat hydrogen in superlattices and show how selective absorption can be used to alter the electronic structure of one of the constituents. The consequences of these modifications will be considered and we will show that, under certain circumstances, hydrogen can be used to tune the dimensionality of the magnetic interactions.

2. Thin films

2.1. Transition metals

Hydrogen is absorbed exothermically by a number of the nonmagnetic transition metals. While the magnetic elements, Cr, Mn, Ni, Fe and Co, only absorb hydrogen endothermically, hydrogen could also be inserted in these elements by, e.g. implantation. The interaction of the energetic ions with the host material, however, inevitably alters the structural quality resulting. No results on reversible tuning of the magnetic properties of thin magnetic films by hydrogen in these elements exist in the literature.

2.2. Rare earth materials

The influence of hydrogen absorption in rare earth (RE) metals has intensively been investigated by a vast number of researchers. A comprehensive review has recently been published [3]. At low concentrations, hydrogen in RE metals can be described as a lattice gas. The metal lattice expands in proportion to the hydrogen concentration, while maintaining its structural and metallic properties (α phase). At higher concentrations a stable dihydride (β) and a trihydride (γ) phases are formed. While most RE metals have a hcp structure, all the dihydrides of trivalent RE metals are fcc. Apart from the divalent REs and the elements La, Ce, and Pr, all lanthanides undergo a second phase transition at higher H content, to the hcp γ-phase.

The magnetic properties of bulk RE metals can be described by localized 4f magnetic moments, which are coupled via a polarization of the 5d and 6s–6p conduction electrons. This type of coupling is referred to as RKKY coupling. In RE metals, the magnetic ordering is therefore governed by the mediation of the coupling through the conduction electron. The RE metals have many different magnetic structures, caused by the filling ratio of the 4f band and the interplay between crystal field and exchange interactions. The influence of hydrogen on the coupling can be viewed as: decreasing the number of electrons in the conduction band through the formation of a sub-band below the Fermi level and modification of the nesting vectors at the Fermi surface.

While the effects of the hydrogen absorption may well take place in bulk materials, realisation of experiments are often hindered by experimental difficulties such as embrittlement and cracking of bulk samples. The synthesis of high quality thin films of pure RE metals, combined with development of optimised hydrogen loading devices, has opened new opportunities. Thin films provide special advantages over bulk materials with respect to their aspect

[1]The hydrogen concentration is defined in terms of hydrogen to metal atomic ratios. Following that convention, 1 corresponds to stoichiometric MH.

ratio, crystal orientation and chemical purity. Molecular beam epitaxy (MBE) is the most commonly used growth technique for RE films and was first explored by Kwo et al. [19] and Durbin et al. [20]. The RE metals can grow epitaxially on sapphire (Al_2O_3) or CaF_2 substrates. A Nb seeding layer is often used to prevent reaction between the RE and the substrate as well as forming a template for the epitaxial growth. REs are extremely reactive, and particularly for thin film samples with a large surface to volume ratio, a reliable method of passivation is required. This is normally achieved by growing approximately 10-nm capping layer of Nb on the films. Although the outermost part of the capping layer is quickly oxidized on exposure to air, the underlying film is protected. To enable in situ loading of the films, the capping layer is often covered by Pd. The surface layer of Pd can easily be activated, allowing fast loading of hydrogen in various experimental environments. The optimal palladium thickness depends on the type of measurements to be performed [21].

The interest in hydrogen in thin RE films is significant, because of the prospect of reversibly tuning the optical, electrical, magnetic, and structural properties of the host metal. As an example, Huiberts et al. demonstrated dramatic changes in resistivity in yttrium hydrides, accompanied by a metal to semiconductor transition [15]. This transition is reversible at room temperature and requires only moderate changes in the gas pressures. Technical applications, such as switchable mirrors, are therefore conceivable. Many experimental and theoretical studies have been devoted to explain the metal–semiconductor transition and the accompanying optical and electrical properties in the YH_x film [15,22–27]. This transition from a metal to a semiconductor implies a complete removal of conduction electrons through the formation of a band gap. Large effects on the magnetic ordering in magnetic RE materials are therefore expected, since the coupling of the magnetic moment is obtained by polarisation of the conduction electrons.

Gadolinium is a good candidate for discussing the influence of hydrogen on the magnetic ordering. The magnetic properties of bulk Gd and its hydrides are well known. Furthermore, finite size and strain effects are expected to play a major role in thin Gd films. Gd is ferromagnetic with a Curie temperature of 293 K. Between 293 and 232 K, the magnetic moment is parallel to the *c* axis; below 232 K it is tilted with respect to the *c* axis, to a maximum tilt of about 65° near 180 K and back to within 32° of the *c* axis at lower temperatures. Systematic differences have been observed in thin films. The magnetic structure of a 500-nm thick Gd film was found to be similar to that of the bulk below 230 K, while the magnetic structures are vastly different above 230 K. In the case of the Gd film the moment direction is constant at 30° with respect to the *c* axis [28]. This difference is directly connected to the shape anisotropy of the film. Fujiki et al. [29] have demonstrated that the direction of the magnetization of a ferromagnet can be canted away from the *c* axis by changing the c/a ratio.

Not only does the absorption of hydrogen cause an hcp to fcc structural transition, it also induces a significant modification of the magnetic properties in the dihydride phase. GdH_2 thin films are antiferromagnets, with a Néel temperature of 22 K. The magnetic properties of GdH_2 thin films are roughly the same as for the $GdD_{1.93}$ bulk sample but are different from those of GdD_2, which has a helical structure [30]. The decrease of the critical temperature induced by the insertion of hydrogen is connected both to a weakening of the magnetic interaction and to a decrease of the effective moment of the Gd atoms. The moment was determined to be 6.3 μ_B in Gd films, while the effective moment was determined to be 3.2 μ_B in GdH_2, which is a questionable result. The changes in the conduction band are expected to alter the coupling and the susceptibility, but not the moment of the localised f-electrons.

Gd trihydride is a semiconducting antiferromagnet, with substantially lower ordering (Néel) temperature ($T_N = 1.8$ K) than Gd [31]. The synthesis of high quality thin films has allowed more detailed investigation of the electronic properties of GdH_3. The band gap energy was found to be approximately 2.5 eV [32,33]. The electronic gap is highly sensitive to the vacancy concentration (vacancy in this context is a missing hydrogen) as well as impurities. In the case of GdH_3, hydrogen absorption gives rise to unexpected magnetic properties. The zero field semiconductor-like behaviour in resistivity was found to be suppressed in a magnetic field of 120 kOe, accompanied with large negative magnetoresistance [34], as seen in Fig. 1.

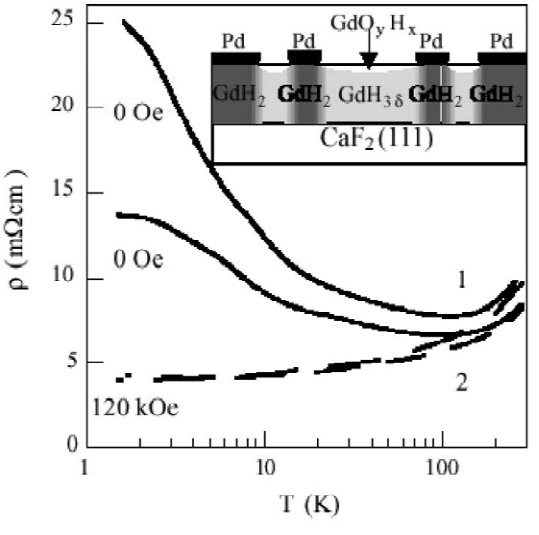

Fig. 1. Temperature dependence of resistivity of GdH_3-thin films with low (1) and high (2) vacancy concentrations in a magnetic field of 120 kOe and in zero field. The inset shows a schematic cross-section of the sample; from Ref. [34].

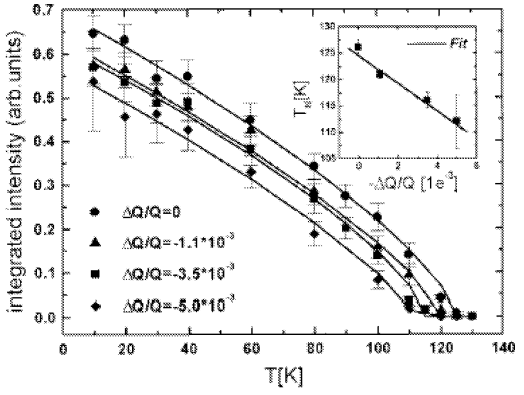

Fig. 2. Temperature dependence of the integrated magnetic scattering intensity of the τ-reflection from the magnetic spiral measured with resonant magnetic X-ray scattering in a thin Ho film for four different hydrogen concentrations. The inset shows the linear reduction of the Néel temperature with increasing hydrogen concentration; from Ref. [18].

The synthesis of thin film sample is also opening opportunities to study RE hydrides with new experimental approaches. For example, resonant magnetic X-ray scattering (XRMS) can be combined with neutron reflectivity to investigate the influence of the hydrogen content on magnetic properties. An incommensurate spin helix below the Néel temperature has been observed in Ho thin films. The average rotation of the moment per plane is characterized by the phase angle $\phi = \tau\pi$ where τ is the wave vector of the magnetic modulation [35]. Sutter et al. have studied the effect of hydrogen content in the α-phase on the magnetic properties of a thin Ho film. They have demonstrated an increase of the spin spiral period with increasing hydrogen concentration, while the Néel temperature decreases (see Fig. 2) [18]. Such investigations are possible because of the chemical purity and well-defined crystalline orientation in the films.

3. Superlattices

An artificial superlattice can be viewed as consisting of artificial unit cells, extending over one period (Λ) defined by the thickness of two different materials layers, as illustrated in Fig. 3. One of the layers can be chosen to be magnetic, being separated by a nonmagnetic layer, giving rise to weakened magnetic interaction in one direction.

It is well known that the ordering temperature decreases as one of the physical dimensions is reduced. In the case of an ideal three-dimensional Heisenberg system, the scaling of the critical Néel- or the Curie-temperature can be expressed as [37]:

$$\frac{T_C(\infty) - T_C(t)}{T_C(\infty)} = bt^{-\lambda} \quad (1)$$

where $T_C(\infty)$ and $T_C(t)$ are the critical temperatures for an infinitely thick film and for a film of finite thickness t,

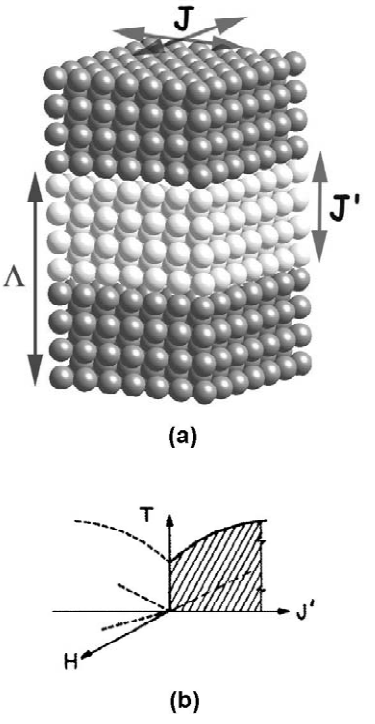

Fig. 3. (a) Illustration of a superlattice with the repeat distance Λ, interlayer coupling J' and an intralayer coupling J; (b) Schematic illustration of the expected ordering temperature with different interlayer coupling; from Ref. [36].

respectively; λ is the shift exponent, which is related to the critical length exponent ν via $\lambda = 1/\nu$. $T_C(t)$ is either the Curie- or the Néel-temperature, depending on the system investigated. Scaling has been observed in the past for a number of thin magnetic films [38]. However, the interplay between scaling and inter-layer coupling has not been investigated so far. The effect of changes in the interlayer coupling on the ordering temperature is minor, as long as $J' \approx J$. But when $J' \ll J$, the ordering temperature for LRO rapidly diminishes. From a theoretical point of view, the critical temperature for a superlattice composed of very thin 2D Heisenberg ferromagnets depends on the ratio of the intra-layer (J) to the inter-layer (J') coupling constant according to [39]

$$T_C \propto \frac{J}{\ln(J/J'')} \quad (2)$$

The investigations of the influence of hydrogen on magnetic interactions in superlattices can be divided into three main categories: (1) both the constituents absorb hydrogen, (2) only the magnetic layers absorb hydrogen, and finally, (3) only the nonmagnetic layers absorb hydrogen. Most of the work has been concentrated on material combinations where only the nonmagnetic component absorbs hydrogen, allowing one to tune selectively the interlayer coupling. This will be treated in more detail below.

3.1. Rare earth based heterostructures

Many RE metals have the same crystal structure with similar lattice constants. Growth of coherent superlattices is therefore possible. In the pioneer work, a variety of superlattices involving magnetic and nonmagnetic heavy RE were grown [19,40] and the list of available materials was extended 10 years later to the light RE elements [41,42]. The preparation of RE superlattices is accomplished using the same architectures and techniques as for thin films (see 2.2) but with an alternating periodic stacking along the growth direction. For a superlattice sample with discrete layers of different materials, a growth temperature is chosen that minimizes interdiffusion at the interfaces, while providing sufficient mobility to promote a layer-by-layer growth. For example, in the MBE growth of Ho–Y superlattices, a temperature between 573 and 673 K was used [43]. Good crystalline quality can be obtained in RE superlattices. Typical mosaicity is around 0.1° and a coherence length can exceed 100 nm perpendicular to the film plane. Interfacial widths can be as low as 2–4 atomic planes.

The RE–Y superlattices have been widely studied, mainly because of the absence of localized magnetic moments in yttrium. The propagation of the magnetic structure through the nonmagnetic Y could thereby be investigated. Yttrium does not have a local moment but very flat Fermi surfaces in the *c* direction, making it an ideal material for mediating interlayer exchange coupling. In fact, in Y the polarized magnetic moment is low but the electron correlation is strong. This effect enables effective propagation of the magnetic ordering, through the Y layers, coherently connecting adjacent blocks of the magnetic material. The coupling scales as the inverse thickness of the Y layers, which is a much slower decay as compared to other common spacer materials.

The Y layers do not simply act as inert spacer in Dy–Y superlattices. A fixed phase shift, proportional to the thickness of the Y block, is observed [44]. A long-range magnetic coherence between adjacent Dy layers is thus stabilized that can extend over many bilayers. A similar feature was observed in the Ho–Y superlattices [43]. The effective turn angle per layer in the Y is the same for several samples, independent of the thickness and temperature. The turn angle in the magnetic material changes with the temperature and is always larger than in bulk samples. This has been linked to strain, imposed by epitaxial growth in the superlattices. The exact mechanism by which the magnetic turn-angle is transmitted across the Y blocks is still to be understood, a stabilization of a helical spin density wave in the Y (turn angle of 52°) conduction electrons has been proposed as a coupling mechanism

Recently, the absorption of hydrogen has been observed in unprotected Nd–Pr superlattices [45]. Within a few months from growth, these light RE samples have been found to react with hydrogen and to form single crystal phases, which are coherent with the overall epitaxial structure. In the case of Ho–Y, both layers can absorb hydrogen. However, at low temperatures, the enthalpy wins over entropy and the hydrogen will reside in the layer with the lower enthalpy of solution. Neutron scattering experiments have shown that this is the Y-layers [18].

It is possible to investigate the modifications of the helical structure in both Ho and Y layers as a function of the thickness by neutron diffraction. This has been done by following the (00τ) magnetic peak position, using the ADAM reflectometer/diffractometer at the Institute Laue-Langevin, Grenoble [46]. For a [Ho(28 ML)–Y(18 ML)]$\times$ 30 superlattice is was shown that the introduction of hydrogen can be used to 'switch off' the interlayer coupling, as seen in Fig. 4. The Néel temperature before and after hydrogen loading remained constant, 118 K, in good agreement with the scaling of the Néel temperature for this particular Ho thickness. No or only little hydrogen enters the Ho layers, because the accompanying reduction of the critical temperature does not occur. Secondly, the suppression of the interlayer coupling does not affect the intralayer ordering temperature, for this Ho thickness. This situation is different for thinner Ho layers, where scaling and dimensional crossover effects become more important. The Néel temperature for a [Ho(10 ML)–Y(25 ML)]$\times$30 superlattice is 94 K for the coupled superlattice without hydrogen and is decreased by 21 K to a Néel temperature of 73 K in the uncoupled case with hydrogen. In fact, this is the same Néel temperature as for the isolated Ho film of the same thickness. This is a clear indication of the importance of the interlayer exchange coupling for the ordering temperature of the Ho layers, when the scaling of the Néel temperature due to finite size effects becomes significant.

RE materials can be combined with TM forming high quality multilayers. Many studies have been devoted to RE–(Fe or Co) because of the peculiar behaviour of interlayer magnetic coupling and magnetic anisotropy (Tb–Fe [47], Nd–Fe [48] for example). While bulk RE metals form stable hydrides, the solubility of hydrogen in bulk transition metals is very low, as stated above (for example -100 kJ/mol H for the formation enthalpy of CeH_2 and $+20$ kJ/mol H for Co in the dilute case [49]). Therefore it is reasonable to assume that only the RE layers absorb hydrogen, i.e. that the growth of [REH_2–(Co or Fe)] multilayers is possible. These artificial structures are fascinating because of the fragile interplay of, e.g. the itinerant Fe and the localised Ce moments. The synthesis is performed using reactive ion beam sputtering of Ce and Co or Fe targets at room temperature using argon in an ultrahigh vacuum chamber, at a hydrogen partial pressure in the 10^{-6} mbar range. High quality CeH_2–Co and CeH_2–Fe multilayers have been obtained with an interfacial width of nominally one atomic layer [50]. The hydrogen free system is spontaneously magnetized in the film plane. On the other hand, in the CeH_2–Fe system with

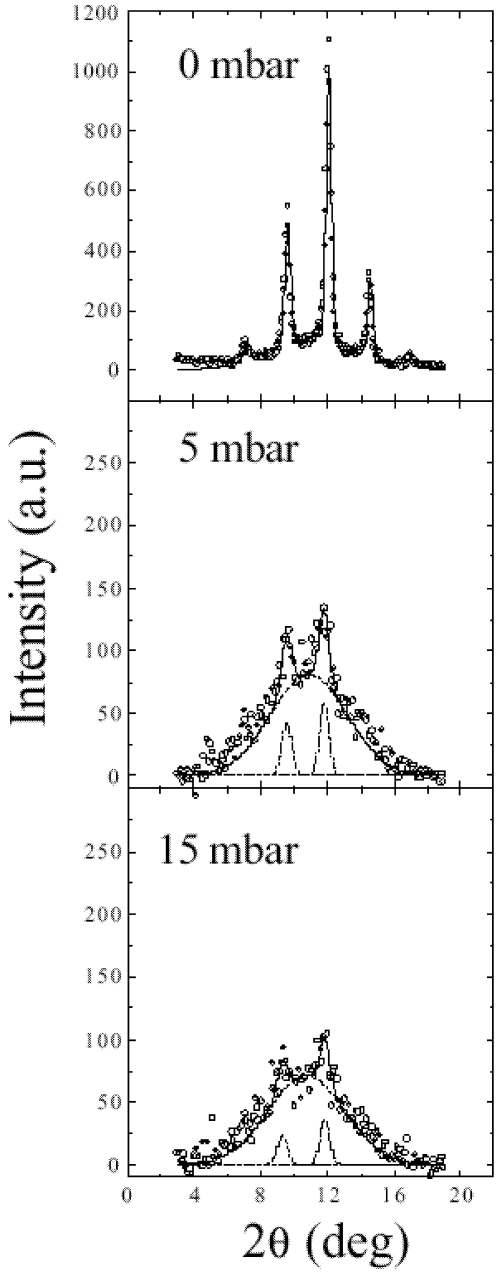

Fig. 4. Magnetic superlattice peaks of the [Ho(10 ML)–Y(25 ML)]×30 superlattice before hydrogen loading (top panel) and after exposure to different hydrogen pressures (middle and bottom panel). The data were taken with neutron scattering at 20 K. The solid lines indicate fits to the data points with Gaussian line shapes of different width and height as indicated by the dashed lines. The weak double spike in the lower panel is reminiscent of the coupled Ho–Y superlattice and indicates a weak residual coupling extending over not more than two Ho blocks.

sufficiently thin Fe layers, the orientation of the spontaneous magnetisation is perpendicular to the film plane at low temperatures and switches abruptly to a parallel alignment at higher temperature. Mössbauer spectroscopy results show that the strong hybridisation between the Ce-5d and Fe-3d states is suppressed upon hydrogenation [51]. The reorientation transition in CeH_2–Fe has been investigated by X-ray magnetic circular dichroism. The role of the spin-split 3d states of the Fe atoms is to induce a magnetic order on the Ce-5d states via hybridisation, even on ions more distant from the interface. Meanwhile, the Ce-4f states have been found to be the root of the reorientation transition. These become magnetically polarized by intra atomic coupling with the Ce-5d states with increasing strength at low temperature and thereby cause the reorientation of the magnetization [52].

3.2. Transition metal based heterostructures

As stated in Section 2.1, the magnetic TM elements do not absorb hydrogen exothermically. Many of the nonmagnetic TM readily absorb hydrogen. The first example of absorbing–nonabsorbing combination, we will discuss is H in Fe–V(001). Fe–V(001) can be grown with epitaxial quality on MgO(001) substrates [53]. The magnetic moment is confined in the plane, showing thickness depending anisotropy. Most of the investigations have been focused on relatively thin Fe layers (around 3 ML) where the anisotropy is small or negligible. The thickness of the V layers is typically in the 3–16 ML range, where the structural quality is the best. Fe–V(001) are FM ordered for V thickness up to 11 ML, in between 12 and 14 ML these are AFM ordered. Samples with thickness of 15 or 16 ML are FM ordered. The dependence of the strength and sign of the inter-layer exchange coupling *J*' on the concentration of H in the V spacer layers was investigated in detail [17]. It is possible to change the IEC from initially FM to AFM as well as FM to AFM ordering, which implies a change of sign in the IEC. The change of sign implies crossing zero, hence, in principle, it should be possible to accomplish arbitrarily small IEC.

When the thickness of the Fe layers is decreased, the ordering temperature is lowered. In Fe(2)–V(13) (001) superlattices, the Néel temperature is 92 K [54]. The reduced ordering temperature is mainly due to the reduced Fe magnetic moment. The average moment, including the AFM aligned V layers at the interfaces, decreased from 1.2 μ_B/Fe-atom in 3 Fe ML to about 0.4 μ_B/Fe-atom in 2 ML samples. The reduced ordering temperature opens up a new route for investigating the influence of hydrogen on the magnetic properties, because a temperature-independent H concentration can be stabilized in the sample. In a first step the sample is loaded with hydrogen at elevated or ambient temperature. Thereafter, the sample is cooled (far below 300 K). This effectively hinders hydrogen absorption–desorption from the sample and thereby the hydrogen concentration is fixed in the sample. In the upper panel of Fig. 5 we show a neutron reflectivity scan for the Fe(2 ML)–V(13 ML) superlattice at 10 K before hydrogen loading. The peak at $2\theta = 5.3°$, half way between the total reflection and the first structural Bragg peak, arises from an anti-parallel alignment of the moments of adjacent Fe layers. The intensity of this peak corresponds to the square

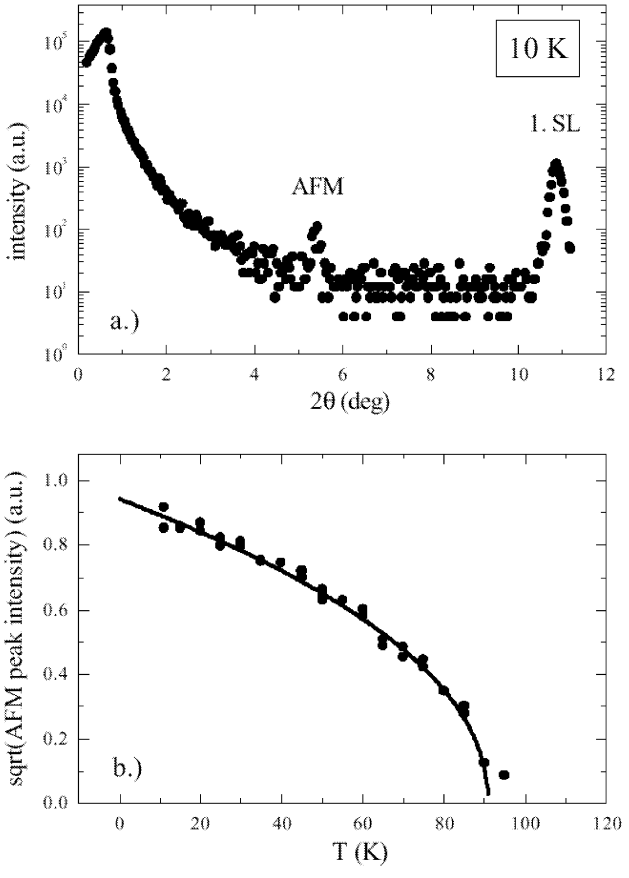

Fig. 5. Top panel: reflectivity curve of the virgin [Fe(2 ML)–V(13 ML)]×200 sample recorded at 10 K. The peak at $2\theta = 11°$ corresponds to the first order superlattice peak and is due to the chemical periodicity. The peak at $2\theta = 5.2°$ indicates a doubling of the magnetic periodicity with respect to the chemical periodicity and is therefore referred to as the AFM peak. Bottom panel: square root of the integrated intensity of the AFM peak as a function of temperature to determine the order parameter and the Néel-temperature ($T \approx 92$ K) of the AFM coupled Fe–V superlattice.

of the order parameter, the temperature-dependence of which is plotted in the lower panel of Fig. 5, showing a Néel temperature of about 92 K for the virgin sample.

The experiment was repeated with different hydrogen concentrations in the V layers. Initially, the AF coupling strength decreases, resulting in a reduction of the Néel-temperature with increasing H content. In Fig. 6 the Néel temperature is plotted as a function of the average lattice expansion, which is proportional to the hydrogen concentration in the V spacer layers. The Néel temperature decreases from 92 K for $\Delta q/q = 0$ and reaches a minimum of 65 K at $\Delta q/q \approx 0.63\%$. Further increase of the hydrogen concentrations leads to a FM ordering with an increasing Curie temperature with increasing $\Delta q/q$. The crossover temperature from AFM to FM coupling is difficult to fine tune and could be even lower than 65 K. The neutron scattering experiments were complemented by SQUID magnetization measurements, in particular in the ferromagnetically coupled region. From both, the neutron and

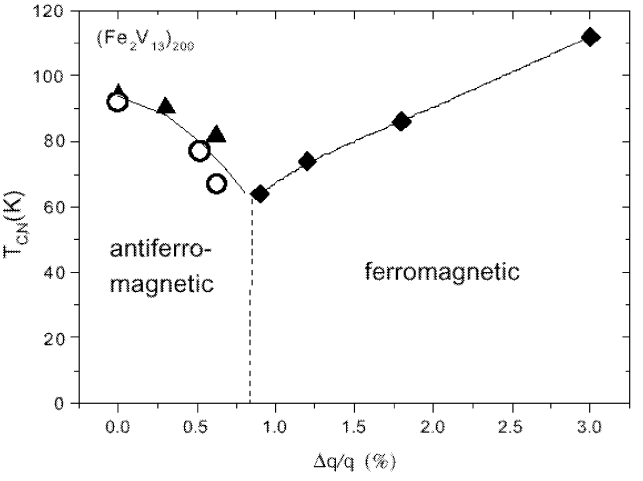

Fig. 6. Néel temperature as a function of the average lattice expansion. The Néel temperature decreases from 92 K for $\Delta q/q = 0$ and reaches a minimum of 65 K at $\Delta q/q \approx 0.8\%$. The hydrogen concentration is proportional to the relative contraction $\Delta q/q$ of the reciprocal lattice. The data are compiled from neutron scattering (open circles) and SQUID measurements (solid triangles and diamonds) [54].

SQUID measurements a phase diagram can be derived for the ordering temperatures as a function of the lattice expansion (hydrogen concentration).

The magnetic susceptibility was investigated using an initially AFM coupled Fe(3 ML)–V(13 ML) sample [55] in an attempt to establish the magnetic phase diagram in the low coupling limit. Strong support for a short-range phase was obtained from the vanishing remnant magnetic moment at temperatures lower than that of the observed maximum in the susceptibility. However, no critical exponent was obtained, which excludes unique determination of the dimensionality of the resulting phases. The principal results are presented in Fig. 7. Since the magnetic moments are confined within the plane, with a very weak in-plane anisotropy, one might speculate that under these conditions a Kosterlitz–Thouless (KT) type phase transition could be observed [56]. The KT transition is characterized by a lack of true long-range translational order. Instead, the correlation function is expected to exhibit an algebraic decay because of the presence of bound vortices, which perturb the long-range positional order. In the present state, however, neither the ordering temperature nor the temperature dependence of the order parameter indicate a KT-type phase transition. Most likely the decoupling at $\Delta q/q \approx 0.8\%$ is not complete and the weak remaining interaction is sufficient to for a 2D–3D crossover, similar to the situation in quasi two-dimensional $CoCl_2$-graphite intercalation compounds [57].

Niobium is in many ways similar to V with respect to hydrogen uptake and interlayer exchange. Nb absorbs hydrogen readily, and magnetic coupling can be mediated through Nb spacers. The use of hydrogen to change the magnetic order in Fe–Nb was pioneered by Klose et al.

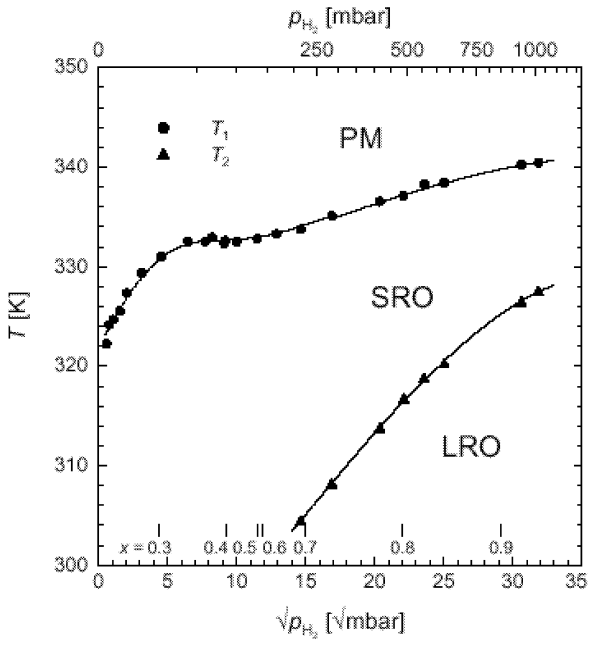

Fig. 7. Changes of the ordering temperature and the topology of the magnetic phases upon insertion of hydrogen in Fe(3)–V(13) (001) superlattice. The sample is initially AFM aligned, the presence of hydrogen switches the magnetic ordering from AFM to FM. The graph shows only the the FM part of the phase diagram (from Ref. [55]).

[16]. A change of the magnetic order was demonstrated utilizing neutron reflectivity measurements. The structural quality of Fe–Nb multilayers is rather poor, due to the large differences of the lattice parameters of the constituents. Large defect density also hinders repeated hydrogen loading of the samples. The second combination utilizing Nb as a spacer, is Co–Nb multilayers. The IEC of Co through NbH_x was investigated by Watts and Rodmacq [58]. The IEC increased upon H insertion and a substantial biquadratic coupling was inferred. The results were discussed within Slonczewski's loose spin model, supporting large magnetic disorder at the interfaces.

Fe, Cr, Co, Pt and Cu do not absorb hydrogen at ambient conditions. Hence, it is not possible to adjust the hydrogen concentration continuously, as described above. Hydrogen can however be inserted by implantation, as described in references [59–61]. The influence of hydrogen implantation on the structural, magnetic and electrical properties of iron–chromium (Fe–Cr) multilayers was investigated by Kandasamy et al. [59]. Hydrogen implantation was found to increase the bilayer thickness, lattice constant, remnant magnetic moment and saturation resistivity. The saturation magnetic field, magnetoresistance and the giant magnetoresistance of the multilayers decreased. Changes in the saturation magnetic moments of multilayers upon hydrogen implantation are also observed. Similar effects were found in Cu–Co [60] and Co–Pt multilayers [61].

4. Summary

We have discussed the possibility of using hydrogen to tune the interlayer exchange coupling in thin films and artificial heterostructures. The change in the coupling and the influence on the magnetic ordering, as well as complete switching of the magnetic order has been described. Not only can the topology of the magnetic ordering be changed, the ordering temperature can be adjusted, through changes in the strength of the IEC. The possibility of using hydrogen to accomplish dimensional crossover is also described.

References

[1] D.E. Bürgler, P. Grünberg, S.O. Demokritov, M.T. Johnson, in: K.H.J. Buschow (Ed.), Handbook of Magnetic Materials, Vol. 13, Interlayer Exchange Coupling in Layered Magnetic Structures, Elsevier, Amsterdam, 2001; in: J.A.C. Bland, B. Heinrich (Eds.), Ultrathin Magnetic Structures I and II, Springer Verlag, Berlin, Heidelberg, New York, 1994.
[2] G. Alefeld, J. Völkl (Eds.), Topics in Applied Physics, Hydrogen in Metals 1 and II, Vol. 29, Springer, Berlin, Heidelberg, New York, 1978, p. 9.
[3] P. Vadja, in: K.A. Gschneidner (Ed.), Handbook on the Physics and Chemistry of Rare Earths. Hydrogen in Rare Earth Metals Including Rh_{2+x} Phases, Vol. 20, Elsevier, Amsterdam, 1995.
[4] H. Zabel, B. Hjörvarsson, in: V.A. Goltsov (Ed.), Progress of Hydrogen Treatment of Materials, International Association for Hydrogen Energy, Donetsk-Coral Gables, 2001.
[5] H. Wagner, H. Horner, Adv. Phys. 23 (1974) 587.
[6] G. Alefeld, Berichte Bunsen-Gesellschaft 76 (1972) 746.
[7] B. Hjörvarsson, J. Rydén, E. Karlsson, J. Birch, J.-E. Sundgren, Phys. Rev. B 43 (1991) 6640.
[8] G. Song, M. Geitz, A. Abromeit, H. Zabel, Phys. Rev. B 54 (1996) 14093.
[9] G. Song, A. Remhof, K. Theis-Brohl, H. Zabel, Phys. Rev. Lett. 55 (1997) 5062.
[10] G. Andersson, B. Hjörvarsson, P. Isberg, Phys. Rev. B 55 (3) (1997) 1774–1781.
[11] G. Andersson, B. Hjörvarsson, H. Zabel, Phys. Rev. B 55 (1997) 15905.
[12] T. Burkert, A. Miniotas, B. Hjörvarsson, Phys. Rev. B 63 (2001) 12 5424/1-5.
[13] Ch. Rehm, H. Maletta, M. Fieber-Erdmann, E. Holub-Krappe, F. Klose, Phys. Rev. B 65 (2002) 113404.
[14] F. Klose, Ch. Rehm, M. Fieber-Erdmann, E. Holub-Krappe, H.J. Bleif, H. Sowers, R. Goyette, L. Trokger, H. Maletta, Physica B 283 (2000) 184.
[15] J.N. Huiberts, R. Griessen, J.H. Rector, R.J. Wijngaarden, J.P. Dekker, D.G. de Groot, N.J. Koeman, Nature 380 (1996) 231.
[16] F. Klose, Ch. Rehm, D. Nagengast, H. Maletta, A. Weidinger, Phys. Rev. Lett. 78 (1997) 1150.
[17] B. Hjörvarsson et al., Phys. Rev. Lett. 79 (1997) 901;
D. Labergerie et al., J. Magn. Magn. Mater. 192 (1999) 238.
[18] C. Sutter, D. Labergerie, A. Remhof, H. Zabel, C. Detlefs, G. Grübel, Europhys. Lett. 53 (2001) 257.
[19] J. Kwo, E.M. Gyorgy, D.B. McWhan, F.J. Disalvo, C. Vettier, J.E. Bower, Phys. Rev. Lett. 55 (1985) 1402.
[20] S.M. Durbin, J.E. Cunningham, J.E. Mochel, C.P. Flynn, J. Phys. F: Met. Phys. 11 (1981) L223.
[21] J.N. Huiberts, J.H. Rector, R.J. Wijngaarden, S. Jetten, D. de Groot,

B. Dam, N.J. Koeman, R. Griessen, B. Hjörvarsson, S. Olafsson, Y.S. Cho, J. Alloys Comp. 239 (1996) 158.
[22] R. Eder, H.F. Pen, G.A. Sawatzky, Phys. Rev. B 56 (1997) 10115.
[23] P.J. Kelly, J.P. Dekker, R. Stumpf, Phys. Rev. Lett. 78 (1997) 1315.
[24] B. Hjörvarsson, J.H. Guo, R. Ahuja, R.C.C. Ward, G. Andersson, O. Eriksson, M.R. Wells, C. Såthe, A. Agui, S.M. Butorin, J. Nordgren, J. Phys.: Condens. Matter 11 (1999) L119.
[25] K.K. Ng, F.C. Zhang, V.I. Anisimov, T.M. Rice, Phys. Rev. B 59 (1999) 5398.
[26] P. van Gelderen, P.A. Bobbert, P.J. Kelly, G. Brocks, Phys. Rev. Lett. 85 (2000) 2989.
[27] M. Rode, A. Borgschulte, A. Jacob, C. Stellmach, U. Barkow, J. Schoenes, Phys. Rev. Lett. 87 (2001) 235502.
[28] S. Hémon, R.A. Cowley, R.C.C. Ward, M.R. Wells, L. Douysset, H. Rönnow, J. Phys.: Condens. Matter 12 (2000) 5011.
[29] N.M. Fujiki, K. De Bell, D.J.W. Geldart, Phys. Rev. B 36 (1987) 8512.
[30] R.R. Arons, J. Schweizer, J. Appl. Phys. 53 (1982) 2645.
[31] R. Carlin, R. Chirico, K. Joung, G. Shenoy, R. Westlake, Phys. Lett. A 75 (1980) 413.
[32] P. van der Sluis, M. Ouwerkerk, P.A. Duine, Appl. Phys. Lett. 70 (1997) 3356.
[33] M.W. Lee, C.H. Lin, J. Appl. Phys. 87 (2000) 7798.
[34] A. Miniotas, P. Norblad, M. Andersson, B. Hjörvarsson, Europhys. Lett. 58 (2002) 442.
[35] G. Helgesen, J.P. Hill, T.R. Thurston, D. Gibbs, J. Kwo, M. Hong, Phys. Rev. B 50 (1994) 2990.
[36] R.B. Griffiths, Phys. Rev. Lett. 24 (1970) 1479.
[37] C. Domb, J. Phys. A 6 (1973) 1296.
[38] Y. Li, K. Baberschke, Phys. Rev. Lett. 68 (1992) 1208.
[39] R.B. Stinchcombe, Phase transitions and dimensionality, in: N.H. March, M.P. Tosi (Eds.), Polymers, Liquid Crystals, and Low Dimensional Solids, Plenum, New York, 1985.
[40] C.F. Majkrzak, J. Kwo, M. Hong, Y. Yafet, D. Gibbs, C.L. Chien, J. Bohr, Adv. Phys. 40 (1991) 99.
[41] B.A. Everitt, J.A. Borchers, M.B. Salamon, J.J. Rhyne, R.W. Erwin, B.J. Park, C.P. Flynn, J. Magn. Magn Mater. 140–144 (1995) 769.
[42] R.C.C. Ward, M.R. Wells, C. Bryn-Jacobsen, R.A. Cowley, J.P. Goff, D.F. McMorrow, J.A. Simpson, Thin Solid Films 275 (1996) 137.
[43] D.A. Jehan, D.F. McMorrow, R.A. Cowley, R.C.C. Ward, M.R. Wells, N. Hagmann, K.N. Clausen, Phys. Rev. B 48 (1993) 5594.
[44] R.W. Erwin, J.J. Rhyne, M.B. Salamon, J. Borchers, S. Sinha, R. Du, J.E. Cunningham, C.P. Flynn, Phys. Rev. B 35 (1987) 6808.
[45] J.P. Goff, C. Bryn-Jacobsen, D.F. McMorrow, R.C.C. Ward, M.R. Wells, Phys. Rev. B 55 (1997) 12537.
[46] A. Schreyer, R. Siebrecht, U. Englisch, U. Pietsch, H. Zabel, Physica B 248 (1998) 349.
[47] Y.J. Wang, W. Keeman, Phys. Rev. B 44 (1991) 5132.
[48] L.T. Baczewski, M. Piecuch, J. Durand, G. Marchal, P. Delcroix, Phys. Rev. B 40 (1989) 11237.
[49] R. Griessen, T. Riesterer, in: L. Schlapbach (Ed.), Hydrogen in Intermetallic Compounds, Vol. 1, Springer, Berlin, 1988, p. 266.
[50] T. Nawrath, B. Damaske, O. Schulte, W. Felsch, Phys. Rev. B 55 (1997) 3071.
[51] P. Bauer, F. Klose, O. Schulte, W. Felsch, J. Magn. Magn. Mater. 138 (1994) 163.
[52] M. Arend, W. Felsch, G. Krill, A. Dellobe, F. Baudelet, E. Dartyge, J.P. Kappler, M. Finazzi, A. San Miguel-Fuster, S. Pizzini, A. Fontaine, Phys. Rev. B 59 (1999) 3707.
[53] J.P. Isberg, B. Hjörvarsson, R. Wäppling, E.B. Svedberg, L. Hultman, Vacuum 48 (1997) 483.
[54] V. Leiner, K. Westerholt, A.M. Blixt, H. Zabel, B. Hjörvarsson, Phys. Rev. Lett., submitted for publication.
[55] T. Burkert, P. Svedling, G. Andersson, B. Hjörvarsson, Phys. Rev. B 66 (R) (2002) 220402.
[56] J.M. Kosterlitz, J. Phys. C 7 (1974) 1046.
[57] D.G. Wiesler, H. Zabel, S.M. Shapiro, Z. Physik B 93 (1994) 274.
[58] R. Watts, B. Rodmacq, J. Magn. Magn. Mater. 174 (1997) 70.
[59] K. Kandasamy, M. Masuda, Y. Hayashi, J. Alloys Comp. 288 (1999) 13.
[60] K. Kandasamy, M. Masuda, Y. Hayashi, J. Alloys Comp. 282 (1999) 23.
[61] Y. Hayashi, M. Masuda, K. Tonomyo, S. Matsumoto, N. Mukai, J. Alloys Comp. 293–295 (1999) 463.